

Maximal work extraction unitarily from an unknown quantum state: Ergotropy estimation via feedback experiments

Jitendra Joshi* and T S Mahesh†

*Department of Physics and NMR Research Center,
Indian Institute of Science Education and Research, Pune 411008, India*

Considering the emerging applications of quantum technologies, studying energy storage and usage at the quantum level is of great interest. In this context, there is a significant contemporary interest in studying *ergotropy*, the maximum amount of work that can be extracted unitarily from an energy-storing quantum device. Here, we propose and experimentally demonstrate a feedback-based algorithm (FQErgo) for estimating ergotropy. This method also transforms an arbitrary initial state to its passive state, which allows no further unitary work extraction. FQErgo applies drive fields whose strengths are iteratively adjusted via certain expectation values, conveniently read using a single probe qubit. Thus, FQErgo provides a practical way for unitary energy extraction and for preparing passive states. By numerically analyzing FQErgo on random initial states, we confirm the successful preparation of passive states and estimation of ergotropy, even in the presence of drive errors. Finally, we implement FQErgo on two- and three-qubit NMR registers, prepare their passive states, and accurately estimate their ergotropy.

I. INTRODUCTION

Quantum technologies are appealing as they can surpass their classical counterparts by using exclusive concepts like coherence and entanglement. Understanding their capabilities has progressed in recent years, thanks to the numerous experimental breakthroughs that have improved control over quantum states. Specifically, the investigation of the principles of quantum thermodynamics is made possible by quantum thermal machines, which include refrigerators and heat engines to regulate heat flow and work production [1, 2]. Further options for storing energy for later extraction include quantum batteries [3–14]. In every possible framework, like charging speed [15–20], stored energy [21, 22], and energy extraction [23–27], the quantum batteries have the potential to outperform their classical counterparts.

The maximum amount of energy that can be extracted from quantum systems through unitary processes is known as *the ergotropy* [28]. A practical way to determine ergotropy is by finding the optimal unitary operation that transforms the system to its lowest attainable energy state, known as its *passive state* [29]. This can be a challenging undertaking as ergotropy might be sensitive to correlations that can also impact device performance [30–37]. Recent works have tried to establish a link between entanglement and thermodynamic quantities like the ergotropy gap, the difference between the maximal extractable works via global and local unitaries. These thermodynamic quantities can be used to verify entanglement present in bipartite [38], multipartite [39, 40], and multiqubit mixed states [41]. Using these quantities, experimental certification of entanglement has been demonstrated in up to 10 qubits [41].

The main focus of this work is FQErgo, an algorithm we propose for preparing the passive state and thereby estimating ergotropy. FQErgo is inspired by (hence the name) the feedback-based algorithm for quantum optimization (FALQON) [42], which has been recently developed for combinatorial quantum optimization. This method uses feedback conditioned on qubit measurements at each quantum circuit layer and parametrized quantum circuits to determine the values of the circuit parameters at subsequent layers. FALQON is related to quantum Lyapunov control (QLC), a feedback procedure to find the controls needed to manipulate a quantum system’s dynamics in a desired way [43, 44].

We note several salient features of the FQErgo algorithm. Firstly, the all-quantum nature of the algorithm: unlike the previous methods [45, 46] for estimating ergotropy, FQErgo requires no classical optimizer. Secondly, FQErgo is robust against circuit errors since each feedback iteration readjusts the drives based on previous errors. This way, cumulative error growth is prevented. Thirdly, the circuit parameters can be read efficiently via an ancillary probe qubit using the interferometric method [47–49]. This way alleviates the need for resource-intensive quantum state tomography. Lastly, being a feedback-based method, FQErgo can be fully automated for convenient practical realizations. In this work, after numerically analyzing the FQErgo algorithm, we experimentally demonstrate it using two and three-qubit NMR registers.

This article is organized as follows. In Sec. II, we describe the theoretical construction of FQErgo algorithm. In Sec. III, we numerically analyze FQErgo over random sets of initial states in one and two-qubit systems. The NMR implementations of FQErgo for both one and two-qubit systems with an additional probe qubit are reported in Sec. IV. Finally, Sec. V summarizes the results and discusses their importance.

* jitendra.joshi@students.iiserpune.ac.in

† mahesh.ts@iiserpune.ac.in

II. THEORY

A. Unitary extraction of work, passive state, and ergotropy

Given a quantum system in a state ρ_0 , the *ergotropy* quantifies the maximum amount of work that is unitarily extracted while leaving the system into a passive state ρ^p from which no further work can be unitarily extracted [28]. If H_0 is the system Hamiltonian, the ergotropy is given by

$$\begin{aligned} \mathcal{E}(\rho_0) &= E(\rho_0) - E(\rho^p), \text{ where,} \\ E(\rho^p) &= \min_U \text{Tr}(U\rho_0U^\dagger H_0). \end{aligned} \quad (1)$$

Let \mathcal{U}_p corresponds to the unitary that minimizes the system energy such that $\rho^p = \mathcal{U}_p\rho_0\mathcal{U}_p^\dagger$ is the passive state [28, 29]. If H_0 and ρ_0 , in their respective eigenbases, are in the form

$$\begin{aligned} H_0 &= \sum_k E_k |E_k\rangle\langle E_k|, \text{ with } E_1 \leq E_2 \leq \dots \text{ and} \\ \rho_0 &= \sum_j r_j |r_j\rangle\langle r_j|, \text{ with } r_1 \geq r_2 \geq \dots, \end{aligned} \quad (2)$$

then the passive state is uniquely defined in the energy eigenbasis as

$$\rho^p = \sum_j r_j |E_j\rangle\langle E_j|. \quad (3)$$

While the above definitions of the passive state and ergotropy are simple and clear, the experimental realization of the passive state from an unknown initial state and thereby estimating its ergotropy has not been reported. In the following, we describe a robust method for the same.

B. FQErgo: A feedback algorithm for ergotropy estimation

FQErgo is based on the FALQON algorithm proposed recently [42]. We assume multiple copies of individually accessible systems each prepared in the state ρ_0 , which is not necessarily known. Alternatively, we assume a quantum system that can be repeatedly prepared into the same unknown state ρ_0 . On introducing a drive Hamiltonian $\beta(t)H_d$, the system evolves as

$$\frac{d}{dt}\rho(t) = i[H_0 + \beta(t)H_d, \rho(t)], \quad (4)$$

where $\beta(t)$ is the time-dependent drive parameter. Here and in the rest of the paper we have set $\hbar = 1$. We seek to minimize the system energy $E(\rho(t)) = \langle H_0 \rangle_{\rho(t)} = \text{Tr}(H_0\rho(t))$, which can be accomplished by designing con-

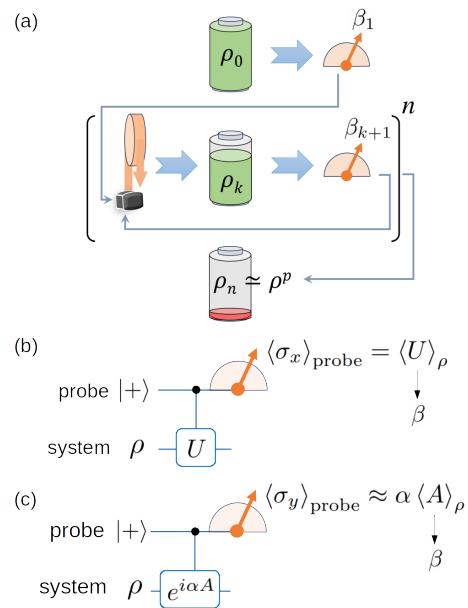


FIG. 1. (a) Illustrating FQErgo taking an initial state ρ_0 in n iterations to $\rho_n \approx \rho^p$, its passive state. (b,c) Determining FQErgo drive amplitude β with a probe qubit, for unitary Hermitian drive σ_γ (b), and nonunitary Hermitian drive A (c). For energy measurement, we set $A = H_0$.

trol $\beta(t)$ such that

$$\forall t \geq 0, \quad \frac{d}{dt} \langle H_0 \rangle_{\rho(t)} = \beta(t) \langle C_d \rangle_{\rho(t)} \leq 0, \quad (5)$$

where $C_d = i[H_d, H_0]$. One way to satisfy the above is by choosing the control in the form [42]

$$\beta(t) = -w \langle C_d \rangle_{\rho(t)}, \quad (6)$$

where w is a positive scalar coefficient.

The overall algorithm is illustrated in Fig. 1 (a). We apply discrete drives each of duration τ and realize a n -step feedback loop,

$$U_n = u_n \cdots u_2 u_1, \text{ with } u_k = e^{-i\beta_k \tau H_d}. \quad (7)$$

We find the first drive parameter by measuring the expectation value $\beta_1 = -w \langle C_d \rangle_{\rho_0}$, and prepare the state $\rho_1 = U_1 \rho_0 U_1^\dagger$. The subsequent steps involve finding

$$\beta_k = -w \langle C_d \rangle_{\rho_{k-1}} \text{ and preparing } \rho_k = U_k \rho_0 U_k^\dagger. \quad (8)$$

Thus, starting from an unknown quantum state ρ_0 , using the sequence of feedback-designed operators $U_n \approx \mathcal{U}_p$, we attain the minimum saturated energy state $\rho_n \approx \rho^p$. The energy measurements of the system for the initial state ρ_0 and the final state $\rho_n \sim \rho^p$ yield an estimation of ergotropy via Eq. 1.

C. FQErgo using a probe qubit

FQErgo described above needs an efficient method to repeatedly extract expectation values of the commutator in Eq. 6, and to monitor the system-energy. Since quantum state tomography is prohibitively expensive for such a task, we shall use the interferometric circuit with an ancillary probe qubit [45–47]. The interferometric circuit for measuring the energy $E(\rho_k)$ as well as extracting the drive parameter β_k in Eq. 8 are shown in Fig. 1 (b,c). The circuit involves preparing the probe qubit in the $|+\rangle$ state, the system in any state ρ , applying a certain controlled operation on the system, and finally measuring the probe qubit. First, consider extracting the expectation value $\langle U \rangle_\rho$ of a unitary Hermitian observable U . In this case, we implement a controlled U gate as shown in Fig. 1 (b). The probe signal is then given by,

$$\langle \sigma_x \rangle_{\text{probe}} = \langle U \rangle_\rho. \quad (9)$$

Thus, we directly obtain the desired expectation value of the system as the signal $\langle \sigma_x \rangle_{\text{probe}}$ in the probe qubit. For example, if the system Hamiltonian is the Pauli operator σ_z as described later in the experimental section, the probe signal directly yields the expectation value $\langle \sigma_z \rangle_\rho$. For the more general case of extracting the expectation value $\langle U \rangle_\rho$ of a nonunitary Hermitian observable A , we construct a unitary $e^{-i\alpha A}$, where α is a scalar parameter such that $\|\alpha A\| \ll 1$. Now implementing the controlled gate as shown in Fig. 1 (c), we obtain the probe signal

$$\langle \sigma_y \rangle_{\text{probe}} = -\langle \sin(\alpha A) \rangle_\rho \approx -\alpha \langle A \rangle_\rho. \quad (10)$$

Here, by setting $A = C_d$, we can extract $\langle C_d \rangle_\rho$ directly as the probe signal $\langle \sigma_y \rangle_{\text{probe}}$.

III. NUMERICAL SIMULATIONS

A. Single qubit system

We consider a single qubit system with Hamiltonian $H_0 = \omega_0(\mathbb{I} - \sigma_z)/2$ with energy eigenvalues $(0, \omega_0)$ prepared in an arbitrary mixed state $\rho(0) = (1 - \epsilon)/2\mathbb{I} + \epsilon|\psi\rangle\langle\psi|$, where $|\psi\rangle = \cos(\theta/2)|0\rangle + e^{i\phi}\sin(\theta/2)|1\rangle$ and the purity parameter $\epsilon \in [0, 1]$. We now use FQErgo to reach its passive state $\rho^p = (1 - \epsilon)\mathbb{I}/2 + \epsilon|0\rangle\langle 0|$. For the one qubit case, FQErgo needs only two drives: σ_x and σ_y . Fig. 2 (a) shows the energy $E(\rho_k)$ versus iteration number k for a set of 20 random initial states. In all cases, we see monotonically decreasing energy, ultimately approaching their respective passive states for sufficiently large iterations n , i.e., $\rho_n \rightarrow \rho^p$. The difference between the initial energy $E(\rho_0)$ and the final energy $E(\rho_n)$ estimates the ergotropy, i.e., $\mathcal{E}_{\text{est}}(\rho_0) = E(\rho_0) - E(\rho_n)$. The filled circles in Fig. 2 (c), plotting $\mathcal{E}_{\text{est}}(\rho_0)$ vs $\mathcal{E}_{\text{exact}}(\rho_0) = E(\rho_0) - E(\rho^p)$ confirm perfect estimation

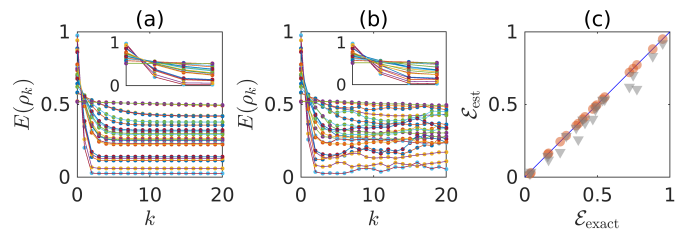


FIG. 2. (a,b) Simulated system-energy $E(\rho_k)$ vs iteration number k for a single qubit ($\omega_0 = 1$) starting from 20 random initial states with ideal FQErgo (a) and FQErgo with random errors (b). Insets show the first three iterations. (c) Numerically estimated vs exact ergotropy values with ideal FQErgo (filled circles) and FQErgo with random errors (filled triangles).

of ergotropy for all the random initial states.

Now we shall analyze the robustness of FQErgo against potential imperfections in practical implementations. Firstly, being a feedback-based method, FQErgo is very robust against the amplitude of the drives. The smaller the drive amplitude, it simply takes longer to reach the passive state. To study the robustness against more general errors, we introduce now an error rotation of 5 degrees about a random direction in every FQErgo iteration. The system-energy curves shown in Fig. 2 (b) do not show perfect monotonic decay, but neither exhibit serious build-up of errors. The corresponding ergotropy values shown by filled triangles in Fig. 2 (c) show somewhat underestimated values, which is expected since circuit errors can make the system settle in only a higher energy state by preventing it from reaching the passive state.

B. Two qubit system

For two or more qubits, energy can be extracted using local unitaries on individual systems or global unitaries on the whole system. If we minimize the system energy using only local unitaries, we can get to *the local passive state* ρ^{pL} , which determines the local ergotropy $\mathcal{E}^L = E(\rho_0) - E(\rho^{pL})$. If we minimize the system energy using global unitaries, along with or without local unitaries, we can get to *the global passive state* ρ^{pG} , which determines the global ergotropy $\mathcal{E}^G = E(\rho_0) - E(\rho^{pG}) \leq E(\rho^{pL})$. The difference $\Delta = \mathcal{E}^G - \mathcal{E}^L$ is called the *ergotropy gap* [50].

Consider a two-qubit system with Hamiltonian $H_0 = \omega_0(\mathbb{I} \otimes \mathbb{I} - (\sigma_z \otimes \mathbb{I} + \mathbb{I} \otimes \sigma_z)/2) + J(\sigma_z \otimes \sigma_z)$ with $|J| \ll |\omega_0|$ and prepared in random initial states $\rho_0^{(12)}$. The ergotropy gap is now

$$\Delta = \mathcal{E}^G(\rho_0^{(12)}) - (\mathcal{E}^L(\rho_0^{(1)}) + \mathcal{E}^L(\rho_0^{(2)})). \quad (11)$$

Our goal is to use FQErgo for estimating both local and global ergotropies and thereby obtaining the ergotropy

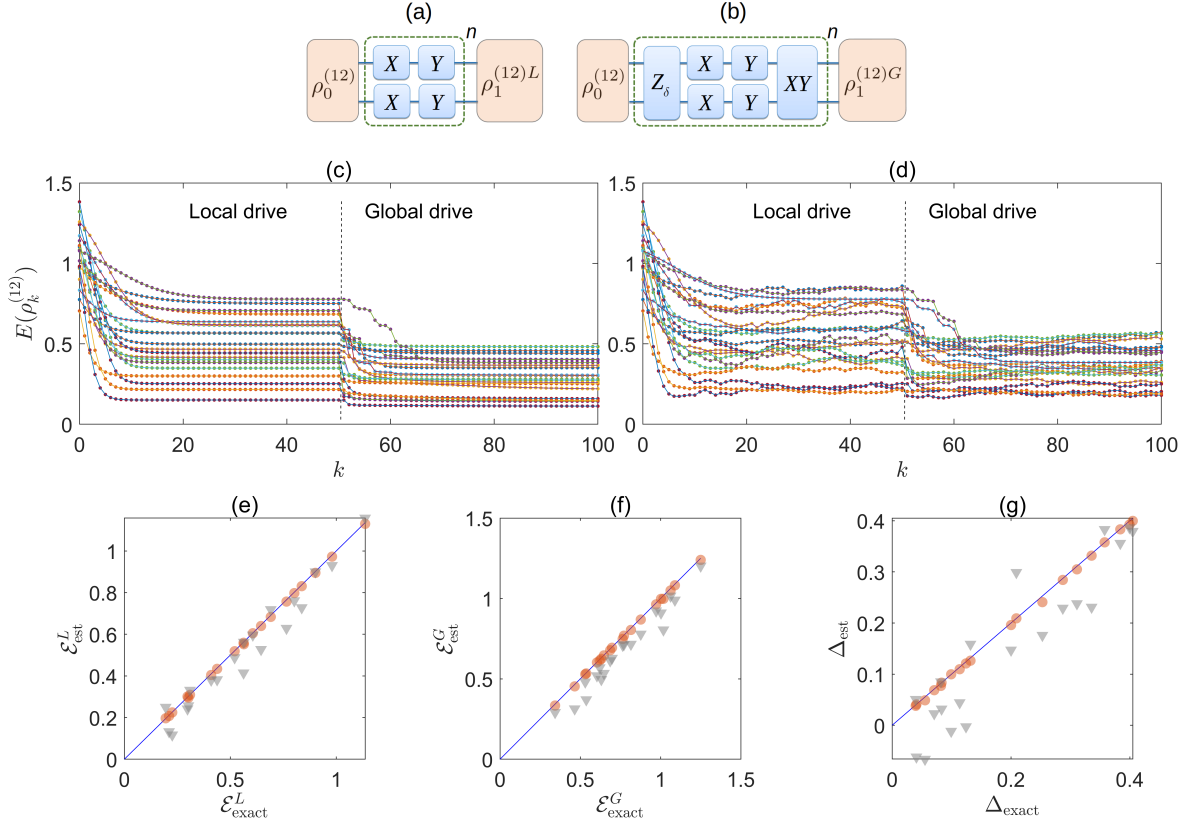


FIG. 3. (a,b) FQergo circuits for local (a) and global (b) energy extraction in two-qubits. Here, local drives X, Y suffice for reaching the local passive state $\rho^{(12)L}$ and estimating the local ergotropy $\mathcal{E}^L(\rho_0^{(12)})$ (a). In contrast, additional global drive such as XY and Z_δ [45] gates are necessary for reaching the global passive state $\rho^{(12)G}$ and estimating the global ergotropy $\mathcal{E}^G(\rho_0^{(12)})$ (b). (c,d) Simulated system-energy vs iteration number for the two-qubit ($\omega_0 = 1$ and $J = 1$) FQergo from 20 random initial states without error (c) and with error (d). (e,f) The numerically estimated local (e) and global ergotropy (f) vs the exact values. (g) Ergotropy gap obtained from (e) and (f), vs the exact values. In (e-g), the filled circles are without random errors and filled triangles are with random errors.

gap. As illustrated in Fig. 3 (a), we use four local drives $H_\gamma^{(1)} = \sigma_\gamma \otimes I$ and $H_\gamma^{(2)} = I \otimes \sigma_\gamma$, where $\gamma \in [x, y]$ over the first 30 iterations that saturated the energy and reached $\rho_{30} \approx \rho^{(12)pL}$, the local passive state. From the 31st iteration, we see a further reduction in energy as we apply a combination of global and local operations, as illustrated in Fig. 3 (b). It involves a tilted phase gate

$$Z_\delta = e^{-i\delta(I \otimes \sigma_y)} \left[|0\rangle\langle 0| \otimes I + |1\rangle\langle 1| \otimes e^{-i\sigma_z \pi/2} \right] e^{i\delta(I \otimes \sigma_y)}$$

with a fixed small angle δ [45], local gates, as well as the global XY gate,

$$U_{xy} = e^{-i\beta_{xy} H_{xy} \tau_{xy}} \text{ with } H_{xy} = \sigma_x \otimes \sigma_y + \sigma_y \otimes \sigma_x,$$

strength β_{xy} , and duration τ_{xy} . Finally, we find the second energy saturation over 60 iterations while reaching $\rho_{60} \approx \rho^{(12)pG}$, the global passive state. Fig. 3 (c) shows the monotonic energy decrease for 20 random initial states undergoing FQergo iteration. For each initial state, we observe two minimum-energy states, one corre-

sponding to the local passive state and the other to the global passive state. Figs. 3 (e-f) plot the estimated local and global ergotropies against their exact values, and Fig. 3 (g) plots the estimated ergotropy gaps against exact values.

We now study FQergo robustness by introducing a random nonlocal error unitary $U_{err} = e^{-iH_{err}\eta}$ generated by a random unit-norm error Hamiltonian H_{err} and $\eta \equiv 2$ degrees in every FQergo iteration. The system-energy curves shown in Fig. 3 (d) lose monotonicity in decay, but retain the overall trend. The error-affected local and global ergotropy values and the corresponding ergotropy gaps are shown by filled triangles in Fig. 3 (e-g). Likewise in one qubit case, the ergotropy values, particularly the global ergotropy values are underestimated, but the rms deviation of the ergotropy gap estimations from the ideal values remains below 0.07 indicating reasonable robustness of FQergo against local/nonlocal errors.

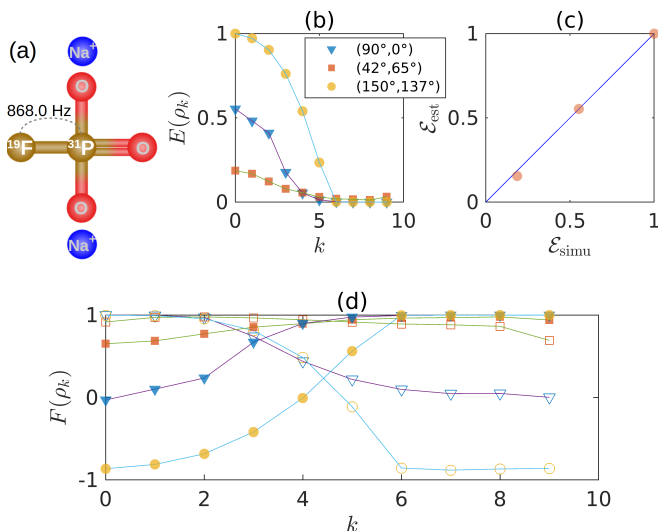


FIG. 4. (a) Sodium fluorophosphate molecular structure with J_{FP} indicated. (b) The experimentally measured one-qubit energy (normalized) vs FQErgo iterations for three initial states $\rho_{\theta,\phi} = U_{\theta,\phi}|00\rangle\langle 00|U_{\theta,\phi}^\dagger$ prepared by one of the RF rotations $U_{\theta,\phi} = e^{-i\theta(I_x \cos \phi + I_y \sin \phi)} \equiv (\theta, \phi)$ as indicated. (c) Ergotropy estimated from (b) vs simulated values. (d) Decaying fidelities of initial states (open symbols) and corresponding growth of passive states (filled symbols) for the same three cases as in (b).

IV. EXPERIMENTS

A. Single-qubit ergotropy

We now use sodium fluorophosphate (dissolved in D_2O ; Fig. 4(a)) as the two-qubit register, wherein ^{19}F is our probe qubit and ^{31}P is the system qubit. All the experiments were carried out on a 500 MHz Bruker NMR spectrometer at an ambient temperature of 300 K. The rotating frame Hamiltonian of the system consisting of the internal part and the RF drive is $H^{FP} = H_{\text{int}}^{FP} + H_{\text{RF}}^{FP}(t)$, where $H_{\text{int}}^{FP} = -\omega_F I_z^F - \omega_P I_z^P + 2\pi J_{FP} I_z^F I_z^P$ and $H_{\text{RF}}^{FP}(t) = \Omega_F(t) I_x^F + \Omega_P(t) I_x^P$, where $I_{x,y,z}$ are the spin operators. Here (ω_F, ω_P) and $(\Omega_F(t), \Omega_P(t))$ respectively denote the adjustable frequency offsets and time-dependent RF amplitudes of ^{19}F and ^{31}P spins, and $J_{FP} = 868.0$ Hz is the scalar coupling constant.

The pulse sequences for the NMR implementations of FQErgo are described in Appendix. Starting from the thermal state, we prepare a pseudopure state (PPS) before energizing the system qubit ^{31}P into one of the three initial states ρ_0 as described in Fig. 4. For FQErgo, we choose the drives I_x and I_y , and their strengths in the k th iteration are given by $\beta_{x(y)} = \langle i[H_0, I_{x(y)}] \rangle_{\rho_{k-1}}$. Notice that all three different states reach their common passive state within 10 iterations in Fig. 4 (b). The corresponding ergotropy values show excellent agreement with the numerically simulated values in Fig. 4 (c), thus demon-

strating the successful implementation of FQErgo.

In this one qubit case, since we have now measured all three expectation values $\langle \sigma_{x,y,z} \rangle_{\rho_k}$, we can now reconstruct the density matrix and determine its state fidelities $F(\rho_k) = \text{Tr}(\rho_0 \rho_k)$ with the respective initial state and $F(\rho_k) = \text{Tr}(\rho_0 \rho_p)$ with the expected target passive state, at each iteration. The resulting fidelity profiles are shown in Fig. 4 (d). They indicate the gradual decay of the initial state fidelity and the corresponding buildup of the passive state fidelity. We clearly find high-fidelity passive states being prepared in each of the three cases.

B. Two-qubit ergotropy

To estimate two-qubit ergotropy, we use the three-spin NMR register dibromofluoromethane (dissolved in Acetone- D_6 ; Fig. 5 (a)). We consider ^{13}C as the probe and 1H , ^{19}F as the system qubits. The rotating frame Hamiltonian consisting of the internal part and the RF drive reads as $H^{\text{CHF}} = H_{\text{int}}^{\text{CHF}} + H_{\text{RF}}^{\text{CHF}}(t)$, where $H_{\text{int}}^{\text{CHF}} = -\omega_C I_z^C - \omega_H I_z^H - \omega_F I_z^F + 2\pi J_{CH} I_z^C I_z^H + 2\pi J_{CF} I_z^C I_z^F + 2\pi J_{HF} I_z^H I_z^F$ and $H_{\text{RF}}^{\text{CHF}}(t) = \Omega_C(t) I_x^C + \Omega_H(t) I_x^H + \Omega_F(t) I_x^F$. Here $(\omega_C, \omega_H, \omega_F)$ and $(\Omega_C, \Omega_H, \Omega_F)$, respectively denote the frequency offsets and RF amplitudes, while (J_{CH}, J_{CF}, J_{HF}) denote the scalar coupling constants, whose values are shown in Fig. 5 (a).

To demonstrate local and global ergotropy estimation, we prepare five initial states with varying degrees of entanglement between the system qubits H and F. The full NMR pulse-sequences are described in the Appendix. After preparing $|000\rangle\langle 000|$ we transform it to $|0\rangle\langle 0| \otimes \rho_0^{\text{HF}} = |0\rangle\langle 0| \otimes U_G|00\rangle\langle 00|U_G^\dagger$ using a global unitary U_G consisting of a Hadamard operator on H and a controlled $e^{-i\nu I_x}$ gate on F. Note that the parameter ν controls the degree of entanglement. That completes the initialization, and now we start work extraction by FQErgo. During the first 10 iterations, we extract work by using only local drives $I_{x(y)}^H, I_{x(y)}^F$ (similar as in Fig. 3 (a)) and realize the first energy minimization corresponding to the local passive state as shown in Fig. 5 (c). From 11th to 20th iterations, we extract further energy via the global drive $I_x^H I_y^F + I_y^H I_x^F$ along with the Z_δ gate and local drives as shown in Fig. 3 (b). The global drive allows complete work extraction, eventually taking the system qubits to the second energy minimization corresponding to the global passive state ρ_{HF}^p . Fig. 5 (b) shows the normalized energies for both local and global extraction with initial states having varying entanglement entropy $S = -\text{Tr}[\rho_0^{\text{HF}} \log \rho_0^{\text{HF}}]$, where $\rho_0^{\text{HF}} = \text{Tr}_F(\rho_0^{\text{CHF}})$. Fig. 5 (c-d) plot the experimentally estimated local and global ergotropy values vs simulated values and Fig. 5 (e) plots the experimentally obtained ergotropy gaps vs versus the simulated values. The good agreement between the estimated values and the simulated values confirms the successful demonstration of the FQErgo algorithm.

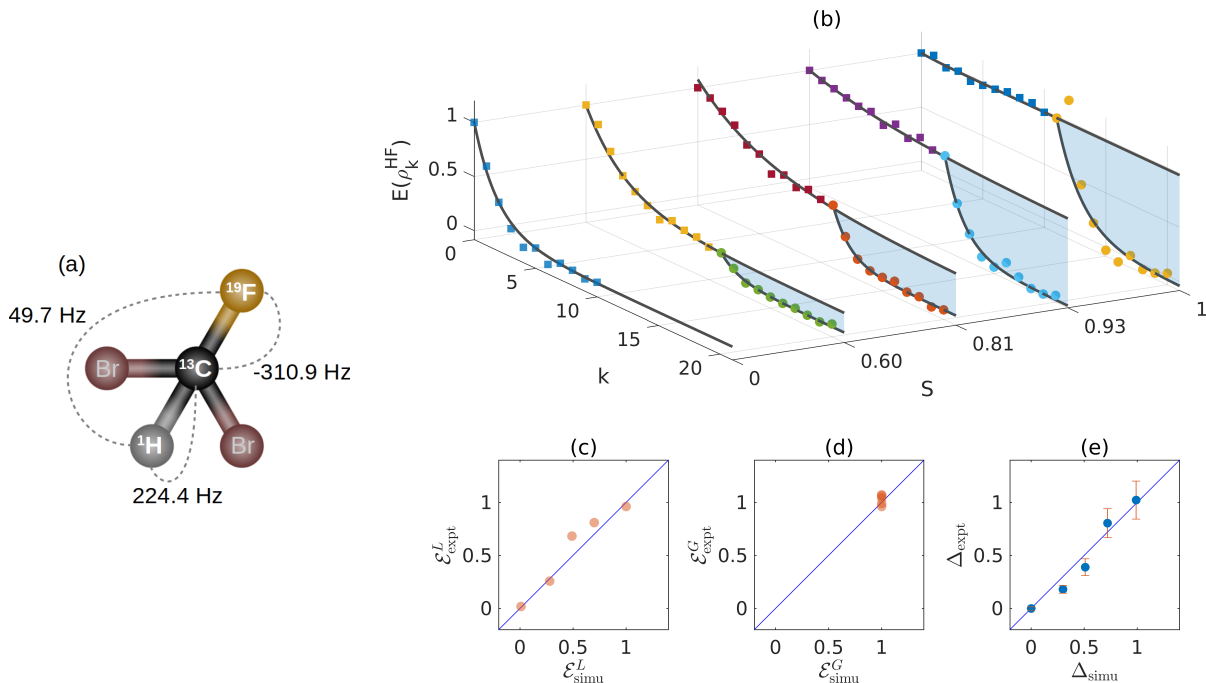


FIG. 5. (a) Molecular structure of dibromofluoromethane, with various J couplings indicated. (b) The experimentally measured two-qubit energy (normalized) vs FQergo iterations for five initial states with varying entanglement entropy (S) as described in the text. (c,d) Local (c) and global (d) ergotropy experimentally estimated from (b) vs simulated values. (e) The experimental ergotropy gap obtained from (c,d) vs simulated values.

V. SUMMARY AND DISCUSSIONS

In summary, we have introduced a feedback-based algorithm, FQergo to prepare the passive state and thereby quantify the ergotropy, the maximum unitarily extractable energy, of an unknown quantum state of a given system. It is an iterative feedback algorithm that efficiently reads certain expectation values using a probe qubit and readjusts the subsequent drive strengths to extract further energy. The same probe qubit also allows regular monitoring of system energy throughout the process. By numerically implementing FQergo over a set of random states in both one and two-qubit systems, we have verified robust passive state preparation and ergotropy estimation, even in the presence of circuit errors. We then experimentally implemented FQergo on multiple initial states of two and three-qubit NMR registers, successfully prepared their passive states, and closely estimated their local and global ergotropies as well as the ergotropy gap.

We envisage several future directions. For instance, previously using ergotropy as an entanglement witness required prior knowledge of the class of states (eg. [41]). FQergo can overcome such limitations and pave the way

to certify the entanglement for a completely unknown state. Since one probe-qubit suffices, irrespective of the system size, extending FQergo to larger systems should be feasible without exponential complexity. Although the ensemble nature of NMR is advantageous here, the overall algorithm is general enough to adapt to other quantum architectures.

ACKNOWLEDGEMENTS

Authors acknowledges valuable discussions with Pranav Chandarana, Mir Alimuddin, Vishal Varma, Arijit Chatterjee, Harikrishnan, and Conan Alexander. J.J. acknowledges support from CSIR (Council of Scientific and Industrial Research) Project No. 09/936(0259)/2019 EMR - I. We also thank the National Mission on Interdisciplinary Cyber-Physical Systems for funding from the DST, Government of India, through the I-HUB Quantum Technology Foundation, IISER-Pune and funding from DST/ICPS/QuST/ 2019/Q67.

APPENDIX: NMR PULSE SEQUENCES

[1] Ronnie Kosloff and Amikam Levy. Quantum heat engines and refrigerators: Continuous devices. *Annual review of*

physical chemistry, 65(1):365–393, 2014.

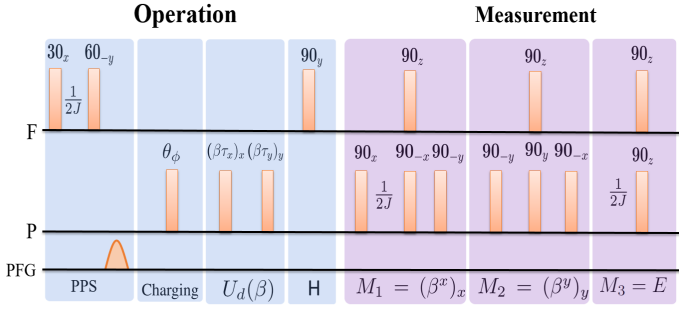


FIG. 6. NMR pulse sequence for the 1-qubit FQERgo experiment. From thermal equilibrium state, we first prepare the $|00\rangle$ pseudopure state (PPS) which is rotated by θ_ϕ to realize the initial state $\rho(0)$. After FQERgo iterations $U_d(\beta)$ on the system qubit ^{31}P (only one iteration is shown) and Hadamard gate (H) on the probe, we extract (i) one of the drive amplitudes $\beta_{x(y)}$ or (ii) energy E . Here the measurement pulse-sequences implement one of $e^{-i\beta^{x/y/z}H_{x/y/z}\tau}$ acting on system ^{31}P qubit and controlled by ^{19}F qubit. Finally, σ_x measurements of ^{19}F qubit yields drive amplitudes $\beta_{x(y)}$ or energy E .

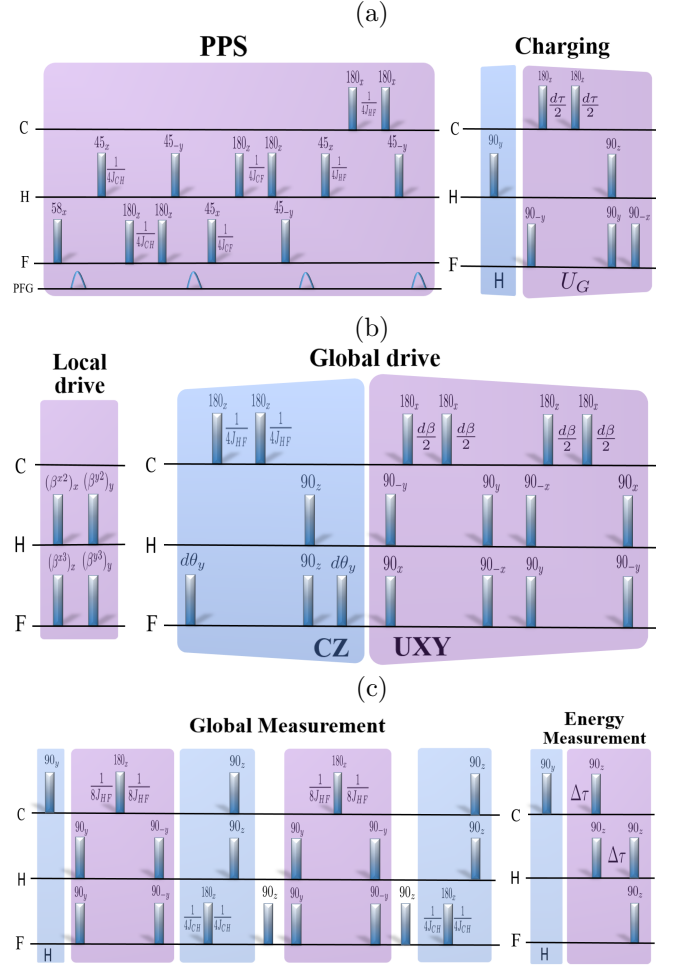


FIG. 7. The NMR pulse sequences for 2-qubit (^1H , ^{19}F), FQERgo with one (^{13}C) probe qubit: (a) PPS preparation, initializing the system as $\rho_{23}(0)$ using entangling unitary U_G after a pseudo-Hadamard on ^1H . Here delay $d\tau$ is varied to change entanglement entropy. (b) Local and global drives, where $UXY = e^{-i\beta^{xy}H_{dxy}\tau}$ and the delay $d\beta$ controls the strength of the global drive. (c) Extracting global drive strength β^{xy} and system energy.

- [2] Mark T Mitchison. Quantum thermal absorption machines: refrigerators, engines and clocks. *Contemporary Physics*, 60(2):164–187, 2019.
- [3] Robert Alicki and Mark Fannes. Entanglement boost for extractable work from ensembles of quantum batteries. *Physical Review E—Statistical, Nonlinear, and Soft Matter Physics*, 87(4):042123, 2013.
- [4] Karen V Hovhannisyanyan, Martí Perarnau-Llobet, Marcus Huber, and Antonio Acín. Entanglement generation is not necessary for optimal work extraction. *Physical review letters*, 111(24):240401, 2013.
- [5] Davide Rossini, Gian Marcello Andolina, and Marco Polini. Many-body localized quantum batteries. *Physical Review B*, 100(11):115142, 2019.
- [6] Gian Marcello Andolina, Maximilian Keck, Andrea Mari, Michele Campisi, Vittorio Giovannetti, and Marco Polini. Extractable work, the role of correlations, and asymptotic freedom in quantum batteries. *Physical review letters*, 122(4):047702, 2019.
- [7] RR Rodriguez, Borhan Ahmadi, Gerardo Suárez, Paweł Mazurek, S Barzanjeh, and Paweł Horodecki. Optimal quantum control of charging quantum batteries. *New Journal of Physics*, 26(4):043004, 2024.
- [8] Jitendra Joshi and T. S. Mahesh. Experimental investigation of a quantum battery using star-topology nmr spin systems. *Phys. Rev. A*, 106:042601, Oct 2022. doi:10.1103/PhysRevA.106.042601. URL <https://link.aps.org/doi/10.1103/PhysRevA.106.042601>.
- [9] Chang-Kang Hu, Jiawei Qiu, Paulo JP Souza, Jiahao Yuan, Yuxuan Zhou, Libo Zhang, Ji Chu, Xianchuang Pan, Ling Hu, Jian Li, et al. Optimal charging of a superconducting quantum battery. *Quantum Science and Technology*, 7(4):045018, 2022.
- [10] Tanoy Kanti Konar, Leela Ganesh Chandra Lakkaraju, Srijon Ghosh, and Aditi Sen. Quantum battery with ultracold atoms: Bosons versus fermions. *Physical Review A*, 106(2):022618, 2022.

- [11] Felipe Barra, Karen V Hovhannisyanyan, and Alberto Imparato. Quantum batteries at the verge of a phase transition. *New Journal of Physics*, 24(1):015003, 2022.
- [12] Francesco Campaioli, Stefano Gherardini, James Q Quach, Marco Polini, and Gian Marcello Andolina. Colloquium: quantum batteries. *Reviews of Modern Physics*, 96(3):031001, 2024.
- [13] Francesco Campaioli, Felix A Pollock, and Sai Vinjanampathy. Quantum batteries. *Thermodynamics in the Quantum Regime: Fundamental Aspects and New Directions*, pages 207–225, 2018.
- [14] Felix C Binder, Sai Vinjanampathy, Kavan Modi, and John Goold. Quantacell: powerful charging of quantum batteries. *New Journal of Physics*, 17(7):075015, 2015.
- [15] Gian Marcello Andolina, Maximilian Keck, Andrea Mari, Vittorio Giovannetti, and Marco Polini. Quantum versus classical many-body batteries. *Physical Review B*, 99(20):205437, 2019.

- [16] Srijon Ghosh, Titas Chanda, and Aditi Sen. Enhancement in the performance of a quantum battery by ordered and disordered interactions. *Physical Review A*, 101(3):032115, 2020.
- [17] Lei Gao, Chen Cheng, Wen-Bin He, Rubem Mondaini, Xi-Wen Guan, and Hai-Qing Lin. Scaling of energy and power in a large quantum battery-charger model. *Physical Review Research*, 4(4):043150, 2022.
- [18] Ju-Yeon Gyhm, Dominik Šafránek, and Dario Rosa. Quantum charging advantage cannot be extensive without global operations. *Physical Review Letters*, 128(14):140501, 2022.
- [19] Raffaele Salvia, Martí Perarnau-Llobet, Géraldine Haack, Nicolas Brunner, and Stefan Nimmrichter. Quantum advantage in charging cavity and spin batteries by repeated interactions. *Physical Review Research*, 5(1):013155, 2023.
- [20] Ricard Ravell Rodriguez, Borhan Ahmadi, Pawel Mazurek, Shabir Barzanjeh, Robert Alicki, and Pawel Horodecki. Catalysis in charging quantum batteries. *Physical Review A*, 107(4):042419, 2023.
- [21] Yu-Yu Zhang, Tian-Ran Yang, Libin Fu, and Xiaoguang Wang. Powerful harmonic charging in a quantum battery. *Physical Review E*, 99(5):052106, 2019.
- [22] Gian Marcello Andolina, Donato Farina, Andrea Mari, Vittorio Pellegrini, Vittorio Giovannetti, and Marco Polini. Charger-mediated energy transfer in exactly solvable models for quantum batteries. *Physical Review B*, 98(20):205423, 2018.
- [23] Dario Ferraro, Michele Campisi, Gian Marcello Andolina, Vittorio Pellegrini, and Marco Polini. High-power collective charging of a solid-state quantum battery. *Physical review letters*, 120(11):117702, 2018.
- [24] Thao P Le, Jesper Levinsen, Kavan Modi, Meera M Parish, and Felix A Pollock. Spin-chain model of a many-body quantum battery. *Physical Review A*, 97(2):022106, 2018.
- [25] Salvatore Tirone, Raffaele Salvia, Stefano Chessa, and Vittorio Giovannetti. Work extraction processes from noisy quantum batteries: The role of nonlocal resources. *Physical Review Letters*, 131(6):060402, 2023.
- [26] Jia-Xuan Liu, Hai-Long Shi, Yun-Hao Shi, Xiao-Hui Wang, and Wen-Li Yang. Entanglement and work extraction in the central-spin quantum battery. *Physical Review B*, 104(24):245418, 2021.
- [27] Juliette Monsel, Marco Fellous-Asiani, Benjamin Huard, and Alexia Auffèves. The energetic cost of work extraction. *Physical review letters*, 124(13):130601, 2020.
- [28] Armen E Allahverdyan, Roger Balian, and Th M Nieuwenhuizen. Maximal work extraction from finite quantum systems. *EPL (Europhysics Letters)*, 67(4):565, 2004.
- [29] Wiesław Pusz and Stanisław L Woronowicz. Passive states and kms states for general quantum systems. *Communications in Mathematical Physics*, 58(3):273–290, 1978.
- [30] John Goold, Marcus Huber, Arnau Riera, Lídia Del Rio, and Paul Skrzypczyk. The role of quantum information in thermodynamics—a topical review. *Journal of Physics A: Mathematical and Theoretical*, 49(14):143001, 2016.
- [31] Manabendra N Bera, Arnau Riera, Maciej Lewenstein, and Andreas Winter. Generalized laws of thermodynamics in the presence of correlations. *Nature communications*, 8(1):2180, 2017.
- [32] Gonzalo Manzano, Francesco Plastina, and Roberta Zambrini. Optimal work extraction and thermodynamics of quantum measurements and correlations. *Physical Review Letters*, 121(12):120602, 2018.
- [33] Giuseppe Vitagliano, Claude Klöckl, Marcus Huber, and Nicolai Friis. Trade-off between work and correlations in quantum thermodynamics. *Thermodynamics in the Quantum Regime: Fundamental Aspects and New Directions*, pages 731–750, 2018.
- [34] Giulia Gemme, Michele Grossi, Dario Ferraro, Sofia Vallecorsa, and Maura Sassetti. Ibm quantum platforms: A quantum battery perspective. *Batteries*, 8(5):43, 2022.
- [35] Fu-Quan Dou, Hang Zhou, and Jian-An Sun. Cavity heisenberg-spin-chain quantum battery. *Physical Review A*, 106(3):032212, 2022.
- [36] Fu-Quan Dou, You-Qi Lu, Yuan-Jin Wang, and Jian-An Sun. Extended dicke quantum battery with interatomic interactions and driving field. *Physical Review B*, 105(11):115405, 2022.
- [37] Fu-Quan Dou and Fang-Mei Yang. Superconducting transmon qubit-resonator quantum battery. *Physical Review A*, 107(2):023725, 2023.
- [38] Mir Alimuddin, Tamal Guha, and Preeti Parashar. Bound on ergotropic gap for bipartite separable states. *Phys. Rev. A*, 99:052320, May 2019. doi:10.1103/PhysRevA.99.052320. URL <https://link.aps.org/doi/10.1103/PhysRevA.99.052320>.
- [39] Xue Yang, Yan-Han Yang, Shao-Ming Fei, and Ming-Xing Luo. Multiparticle entanglement classification with the ergotropic gap. *Phys. Rev. A*, 109:062427, Jun 2024. doi:10.1103/PhysRevA.109.062427. URL <https://link.aps.org/doi/10.1103/PhysRevA.109.062427>.
- [40] Samgeeth Puliylil, Manik Banik, and Mir Alimuddin. Thermodynamic signatures of genuinely multipartite entanglement. *Phys. Rev. Lett.*, 129:070601, Aug 2022. doi:10.1103/PhysRevLett.129.070601. URL <https://link.aps.org/doi/10.1103/PhysRevLett.129.070601>.
- [41] Jitendra Joshi, Mir Alimuddin, T. S. Mahesh, and Manik Banik. Experimental verification of many-body entanglement using thermodynamic quantities. *Phys. Rev. A*, 109:L020403, Feb 2024. doi:10.1103/PhysRevA.109.L020403. URL <https://link.aps.org/doi/10.1103/PhysRevA.109.L020403>.
- [42] Alicia B. Magann, Kenneth M. Rudinger, Matthew D. Grace, and Mohan Sarovar. Feedback-based quantum optimization. *Phys. Rev. Lett.*, 129:250502, Dec 2022. doi:10.1103/PhysRevLett.129.250502. URL <https://link.aps.org/doi/10.1103/PhysRevLett.129.250502>.
- [43] Sen Kuang and Shuang Cong. Lyapunov control methods of closed quantum systems. *Automatica*, 44(1):98–108, 2008.
- [44] Shao-Chen Hou, MA Khan, XX Yi, Daoyi Dong, and Ian R Petersen. Optimal lyapunov-based quantum control for quantum systems. *Physical Review A—Atomic, Molecular, and Optical Physics*, 86(2):022321, 2012.
- [45] Duc Tuan Hoang, Friederike Metz, Andreas Thomasen, Tran Duong Anh-Tai, Thomas Busch, and Tomás Fogarty. Variational quantum algorithm for ergotropy estimation in quantum many-body batteries. *Phys. Rev. Res.*, 6:013038, Jan 2024. doi:10.1103/PhysRevResearch.6.013038. URL <https://link.aps.org/doi/10.1103/PhysRevResearch.6.013038>.

- [46] Dominik Šafránek, Dario Rosa, and Felix C. Binder. Work extraction from unknown quantum sources. *Phys. Rev. Lett.*, 130:210401, May 2023. doi: 10.1103/PhysRevLett.130.210401. URL <https://link.aps.org/doi/10.1103/PhysRevLett.130.210401>.
- [47] Osama Moussa, Colm A Ryan, David G Cory, and Raymond Laflamme. Testing contextuality on quantum ensembles with one clean qubit. *Physical review letters*, 104(16):160501, 2010.
- [48] Sharad Joshi, Abhishek Shukla, Hemant Katiyar, Anirban Hazra, and T. S. Mahesh. Estimating franck-condon factors using an nmr quantum processor. *Phys. Rev. A*, 90:022303, Aug 2014. doi: 10.1103/PhysRevA.90.022303. URL <https://link.aps.org/doi/10.1103/PhysRevA.90.022303>.
- [49] TS Mahesh, Abhishek Shukla, Swathi S Hegde, CS Kumar, Hemant Katiyar, Sharad Joshi, and KR Rao. Ancilla assisted measurements on quantum ensembles: General protocols and applications in nmr quantum information processing. *arXiv preprint arXiv:1509.04506*, 2015.
- [50] Martí Perarnau-Llobet, Karen V. Hovhannisyan, Marcus Huber, Paul Skrzypczyk, Nicolas Brunner, and Antonio Acín. Extractable work from correlations. *Phys. Rev. X*, 5:041011, Oct 2015. doi: 10.1103/PhysRevX.5.041011. URL <https://link.aps.org/doi/10.1103/PhysRevX.5.041011>.